The autoimmune targets in IPEX are dominated by gut epithelial proteins

Eriksson, Daniel

2019-07

Eriksson , D , Bacchetta , R , Gunnarsson , H I , Chan , A , Barzaghi , F , Ehl , S , Hallgren , Å , van Gool , F , Sardh , F , Lundqvist , C , Laakso , S M , Rönnblom , A , Ekwall , O , Mäkitie , O , Bensing , S , Husebye , E S , Anderson , M , Kampe , O & Landegren , N 2019 , ' The autoimmune targets in IPEX are dominated by gut epithelial proteins ' , Journal of Allergy and Clinical Immunology , vol. 144 , no. 1 , pp. 327-+ . https://doi.org/10.1016/j.jaci.2019.02.031

http://hdl.handle.net/10138/303947
https://doi.org/10.1016/j.jaci.2019.02.031

2. Martin S, Pombo I, Poncet P, David B, Arock M, Blank U. Immunologic stimulation of mast cells leads to the reversible exposure of phosphatidylserine in the absence of apoptosis. Int Arch Allergy Immunol 2000;123:249-58.
3. Yotsumoto K, Okoshi Y, Shibuya K, Yamazaki S, Tahara-Hanaoka S, Honda S, et al. Paired activating and inhibitory immunoglobulin-like receptors, MAIR-I and MAIR-II, regulate mast cell and macrophage activation. J Exp Med 2003;198:223-33.
4. Nakahashi-Oda C, Tahara-Hanaoka S, Honda S, Shibuya K, Shibuya A. Identification of phosphatidylserine as a ligand for the CD300a immunoreceptor. Biochem Biophys Res Commun 2012;417:646-50.
5. Nakahashi-Oda C, Tahara-Hanaoka S, Shoji M, Okoshi Y, Nakano-Yokomizo T, Ohkohchi N, et al. Apoptotic cells suppress mast cell inflammatory responses via the CD300a immunoreceptor. J Exp Med 2012;209:1493-503.
6. Joulia R, L'Faqihi F-E, Valitutti S, Espinosa E. IL-33 fine tunes mast cell degranulation and chemokine production at the single-cell level. J Allergy Clin Immunol 2017;140:497-509.e10.
7. Irani AA, Schechter NM, Craig SS, DeBlois G, Schwartz LB. Two types of human mast cells that have distinct neutral protease compositions. Proc Natl Acad Sci USA 1986;83:4464-8.
8. Poon I, Lucas C, Rossi A, Ravichandran K. Apoptotic cell clearance: basic biology and therapeutic potential. Nat Rev Immunol 2014;14:166-80.

Available online May 30, 2019.
https://doi.org/10.1016/j.jaci.2019.03.005

The autoimmune targets in IPEX are dominated by gut epithelial proteins

To the Editor:

Regulatory T (Treg) cells play a key role in immune system homeostasis by suppressing detrimental immune responses against self-proteins, in particular in the intestine.[1] Patients with mutations in the gene *FOXP3* display a severe defect of Treg-cell function that results in IPEX syndrome (OMIM 304790) characterized by impaired immune tolerance and multiorgan autoimmunity. Dermatitis, type 1 diabetes, and in particular autoimmune enteropathy are hallmarks of the syndrome. Intestinal Treg cells normally suppress immune responses against harmless dietary antigens and commensal microorganisms, but the intestinal self-proteins that are guarded by Treg cells have not yet been fully identified.[2]

Patients with IPEX and enteritis typically harbor autoantibodies against harmonin (*USH1C*) and villin, which are structural proteins predominantly expressed in brush border epithelia of the intestine and renal tubules.[3,4] Autoantibodies against glutamate decarboxylase-65 (GAD-65, *GAD2*),[5] which is a marker for islet cell autoimmunity in type 1 diabetes, have been detected in patients with IPEX already in their first week of life. These studies suggest that the autoimmune pathogenesis of IPEX involves a humoral response that can be exploited for identifying the immune targets.[6] Hitherto, no studies have been undertaken to characterize autoantigens in IPEX syndrome in a comprehensive way. Here, we sought to identify the autoantibody targets in patients with IPEX on a broad scale to gain better understanding of the autoimmune manifestations of IPEX and insights to peripheral tolerance mechanisms mediated by Treg cells.

We used panels of more than 9000 human proteins to characterize autoantibody targets in 14 patients with IPEX and 24 healthy controls (detailed methodology and additional tables/figures are available in this article's Online Repository at www.jacionline.org). In total 20 proteins clearly stood out as patient-specific autoantigens (Fig 1; see Table E1 in this article's Online Repository at www.jacionline.org). Among them, the 3 previously known IPEX autoantigens included in the panels were all present: harmonin,[3] α-IFN,[7] and GAD-65,[5] verifying a reliable detection of autoantibodies (Fig 1, *C*, and Fig E1).

Interestingly, the new autoantigens showed predominant expression in tissues typically affected in patients with IPEX, in particular in the intestinal epithelium. In the brush border of enterocytes, ANKS4B and harmonin form a complex that anchors transmembrane links reaching between the tips of microvilli to the enterocyte cytoskeleton (Fig 2, *A*). Competition assays revealed no autoantibody cross-reactivity, suggesting that harmonin and ANKS4B were independent autoantigens (see Fig E2 in this article's Online Repository at www.jacionline.org). Another novel autoantigen, ACSL5, is primarily expressed in the small intestine, where it regulates the enterocyte proliferation along the crypt-villus axis. The protein with the strongest autoantibody signal in the protein array data, HNF4A, is a nuclear receptor with an expression pattern that closely follows that of harmonin and ANKS4B. HNF4A has important functions in differentiation of intestinal and renal epithelia. To validate the proteome-wide autoantibody data with an independent method, we developed radio-ligand binding assays for a subset of the new candidate autoantigens ANKS4B, HNF4A, PPARG, and RXRA, as well as for 3 established autoantigens: GAD-65, harmonin, and villin. We extended the group of patients with IPEX with 3 additional patients in the validation experiments (n = 17). To better evaluate the clinical specificity, we also included a larger group of healthy subjects (n = 75) and sera from other autoimmune and inflammatory diseases: inflammatory bowel disease (n = 20), autoimmune polyendocrine syndrome (APS) type 1 (n = 20), and APS-2 (n = 40). The novel autoantigens ANKS4B, HNF4A, PPARG, and RXRA were all confirmed in the radio-ligand binding assay and showed high specificity for IPEX in the investigated clinical material (see Figs E3 and E4 in this article's Online Repository at www.jacionline.org).

Among the 16 patients with IPEX and enteropathy, 11 of 16 (69%) were positive for autoantibodies against harmonin, 9 of 16 (56%) against ANKS4B, 7 of 16 (44%) against HFN4A, and 8 of 14 (57%) against ACSL5 (ACSL5 autoantibody data were available only for the discovery case group) (Fig 2, *B*). Hence, 11 of 16 patients (69%) displayed autoantibodies against 1 or more autoantigens in the intestinal epithelium. Although the number of patients without enteropathy was too small to assess any statistical associations with specific autoantibodies, we noted that the only patient without enteropathy was negative for all the intestinal autoantibodies. Two patients were negative for all investigated autoantibodies. Both these patients displayed clinical manifestations and mutations in FOXP3 typical for IPEX (Table E1).

Besides HNF4A, our list of top 20 targets from the protein array contained 10 additional nuclear receptors, all with highly correlated results. Because nuclear receptors share an evolutionary template featuring a highly conserved DNA-binding domain and a moderately conserved ligand-binding domain, we performed competition assays to test for cross-reactivity. Focusing on a subset of the nuclear receptor autoantigens, HNF4A, RXRA, and PPARG, we could demonstrate a cross-reactivity between these autoantigens (see Fig E5 in this article's Online Repository at www.jacionline.org). Hence, the nuclear receptor autoantibodies were specific for a subset of nuclear receptors, but cross-reactive within this subset. Investigations of

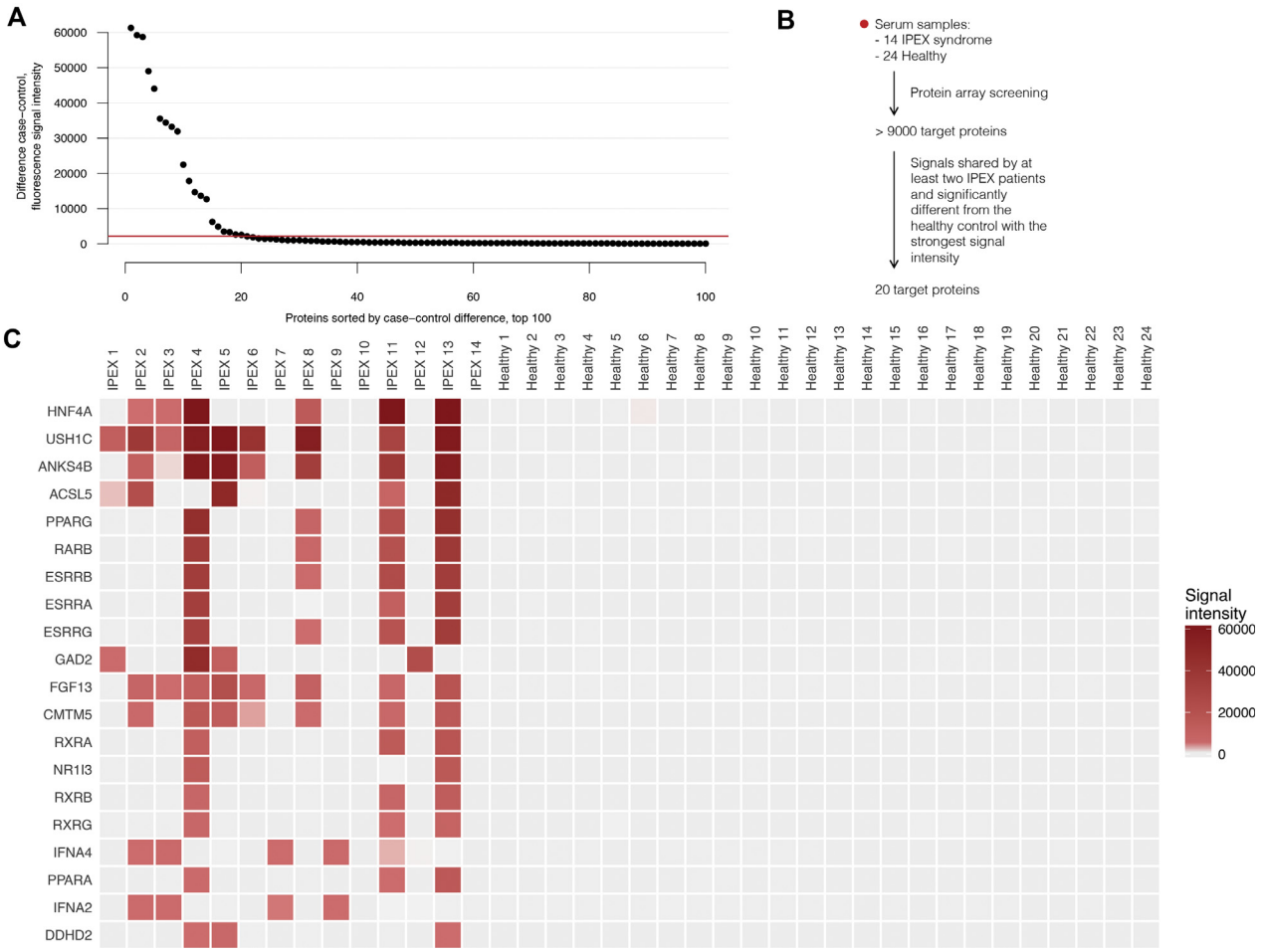

FIG 1. Identification of autoantigens in IPEX by proteome-wide screen. **A** and **B,** To identify IPEX-specific autoantigen signals, the difference in signal intensity between the second to strongest case and the strongest healthy control was calculated for each protein target. A total of 20 protein targets stood out from the background level, delineated by the red line, and were selected for further scrutiny. **C,** The heatmap shows the signal intensities for cases and controls, for the top 20 protein targets.

truncated nuclear receptor protein in the array indicated that the nuclear receptor autoantibodies targeted a shared epitope in the ligand-binding domain.

IPEX can rapidly become fatal if not aggressively treated. Although immunosuppressive therapy can give transient or partial improvement of disease symptoms, allogenic hematopoietic stem cell transplantation (HSCT) offers the only possibility of cure. By investigating consecutive samples from patients with IPEX taken before and after treatment, we found that autoantibodies remained detectable following immunosuppressive treatment with rapamycin but completely disappeared 1.5 years following successful HSCT (see Fig E6 in this article's Online Repository at www.jacionline.org). The replenishment of stem cells with normal functioning FOXP3 might explain disease suppression and disappearance of autoantibodies following HSCT not observed with immunosuppressive treatments.

Although this is by far the most comprehensive study of autoantibody targets in IPEX, less than half of the protein coding genes were covered in our screen. For instance, the previously identified skin autoantigen in IPEX, keratin 14,[8] was not present in the investigated panel.

In summary, we have identified intestinal self-antigens that are implicated in the enteropathy of IPEX, which may advance the understanding of FOXP3-dependent Treg cells in controlling immune tolerance toward self-antigens in the gut.

Daniel Eriksson, MD, PhD[a,b]
Rosa Bacchetta, MD, PhD[c]
Hörður Ingi Gunnarsson, MSc[a]
Alice Chan, MD, PhD[d]
Federica Barzaghi, MD, PhD[e]
Stephan Ehl, MD, PhD[f]
Åsa Hallgren, MSc[a]
Frederic van Gool, PhD[g]
Fabian Sardh, MD[a]
Christina Lundqvist, MD, PhD[h]
Saila M. Laakso, MD, PhD[i]
Anders Rönnblom, MD, PhD[j]
Olov Ekwall, MD, PhD[h,k]
Outi Mäkitie, MD, PhD[i,l,m,n]
Sophie Bensing, MD, PhD[b,l]
Eystein S. Husebye, MD, PhD[a,o,p,q]
Mark Anderson, MD, PhD[g]
Olle Kämpe, MD, PhD[a,b,q]
Nils Landegren, MD, PhD[a,r]

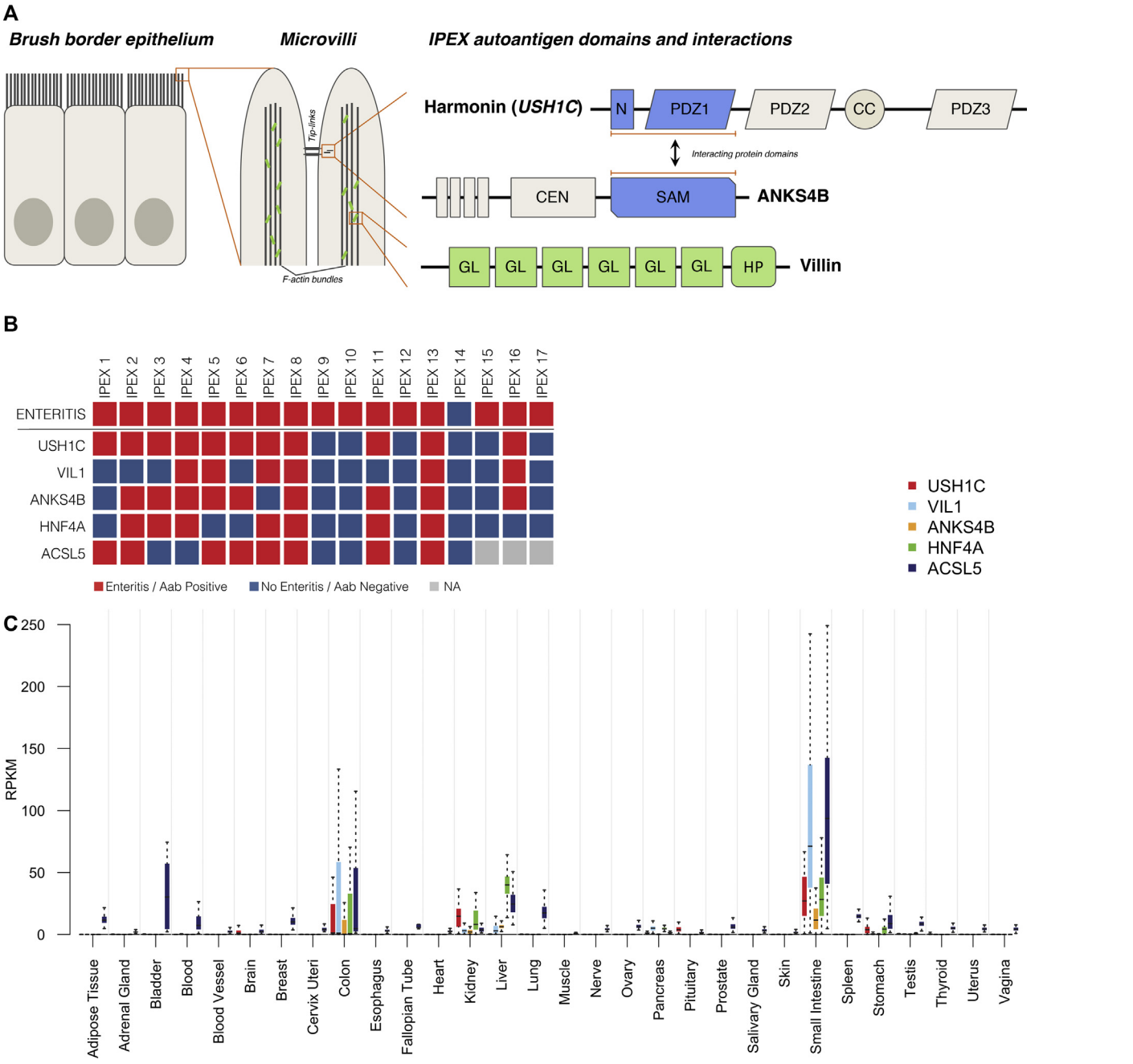

FIG 2. Enterocyte autoantigens in patients with IPEX. **A,** The intestinal epithelium microvilli are interconnected with cadherin tip-links. The previously established autoantigen harmonin and the hereby identified autoantigen ANKS4B are integral parts of a larger complex connecting the transmembrane tip-links to the actin bundles of the cytoskeleton. The interacting domains of harmonin and ANKS4B are highlighted in blue. The established autoantigen villin bundles actin filaments in the intestinal microvilli. **B,** Patients with IPEX and enteritis react with enterocyte autoantigens: Harmonin, villin, ANKS4B, HNF4A, and ACSL5. **C,** IPEX autoantigens show similar profiles of tissue expression. RNA-seq data were obtained from the genotype-tissue expression (GTEx) project. *NA,* Not applicable/available.

From [a]the Center for Molecular Medicine, Department of Medicine (Solna), Karolinska Institutet, Stockholm, Sweden; [b]the Department of Endocrinology, Metabolism and Diabetes, Karolinska University Hospital, Stockholm, Sweden; [c]the Department of Pediatrics, Division of Stem Cell Transplantation and Regenerative Medicine, Stanford University School of Medicine, Stanford, Calif; [d]the Department of Pediatrics, University of California San Francisco, San Francisco, Calif; [e]San Raffaele Telethon Institute for Gene Therapy, Pediatric Immunohematology and Bone Marrow Transplantation Unit, IRCCS San Raffaele Scientific Institute, Milan, Italy; [f]the Center for Chronic Immunodeficiency, Freiburg University Hospital, Faculty of Medicine, University of Freiburg, Freiburg, Germany; [g]the Diabetes Center, University of California San Francisco, San Francisco, Calif; [h]the Department of Rheumatology and Inflammation Research, Institute of Medicine, Sahlgrenska Academy, University of Gothenburg, Gothenburg, Sweden; [i]Children's Hospital, University of Helsinki and Helsinki University Hospital, Helsinki, Finland; [j]the Department of Medical Sciences, Gastroenterology, Uppsala University, Uppsala, Sweden; [k]the Department of Pediatrics, Institute of Clinical Sciences, Sahlgrenska Academy, University of

Gothenburg, Gothenburg, Sweden; [l]the Department of Molecular Medicine and Surgery, Karolinska Institutet, Stockholm, Sweden; [m]the Department of Clinical Genetics, Karolinska University Hospital, Stockholm, Sweden; [n]Folkhälsan Institute of Genetics and University of Helsinki, Helsinki, Finland; [o]the Department of Clinical Science, University of Bergen, Bergen, Norway; [p]the Department of Medicine, Haukeland University Hospital, Bergen, Norway; [q]K.G. Jebsen Center for Autoimmune Disorders, Bergen, Norway; and [r]the Science for Life Laboratory, Department of Medical Sciences, Uppsala University, Uppsala, Sweden. E-mail: daniel.eriksson@ki.se.

This study was funded by the Swedish Research Council, the Torsten and Ragnar Söderberg foundations, the Novo Nordisk Foundation, the Academy of Finland, the Crafoord Foundation, the Folkhälsan Research Foundation, the Helmsley Charitable Trust, the KG Jebsen Foundation, the Marcus Borgström Foundation, the Stockholm County Council, and the Swedish Society for Medical Research.

Disclosure of potential conflict of interest: O. Kampe is a board member of Olink Bioscience. The rest of the authors declare that they have no relevant conflicts of interest.

REFERENCES

1. Tanoue T, Atarashi K, Honda K. Development and maintenance of intestinal regulatory T cells. Nat Rev Immunol 2016;16:295-309.
2. Russler-Germain EV, Rengarajan S, Hsieh CS. Antigen-specific regulatory T-cell responses to intestinal microbiota. Mucosal Immunol 2017;10:1375-86.
3. Kobayashi I, Imamura K, Kubota M, Ishikawa S, Yamada M, Tonoki H, et al. Identification of an autoimmune enteropathy-related 75-kilodalton antigen. Gastroenterology 1999;117:823-30.
4. Kobayashi I, Kubota M, Yamada M, Tanaka H, Itoh S, Sasahara Y, et al. Autoantibodies to villin occur frequently in IPEX, a severe immune dysregulation, syndrome caused by mutation of FOXP3. Clin Immunol 2011;141:83-9.
5. Baekkeskov S, Aanstoot HJ, Christgau S, Reetz A, Solimena M, Cascalho M, et al. Identification of the 64K autoantigen in insulin-dependent diabetes as the GABA-synthesizing enzyme glutamic acid decarboxylase. Nature 1990;347:151-6.
6. Kinnunen T, Chamberlain N, Morbach H, Choi J, Kim S, Craft J, et al. Accumulation of peripheral autoreactive B cells in the absence of functional human regulatory T cells. Blood 2013;121:1595-603.
7. Rosenberg JM, Maccari ME, Barzaghi F, Allenspach EJ, Pignata C, Weber G, et al. Neutralizing anti-cytokine autoantibodies against interferon-α in immunodysregulation polyendocrinopathy enteropathy X-linked. Front Immunol 2018;9:544.
8. Huter EN, Natarajan K, Torgerson TR, Glass DD, Shevach EM. Autoantibodies in scurfy mice and IPEX patients recognize keratin 14. J Investig Dermatol 2010;130:1391-9.

Available online April 23, 2019.
https://doi.org/10.1016/j.jaci.2019.02.031

Mast cell recruitment is modulated by the hairless skin microbiome

To the Editor:

Mast cells (MCs) are abundant in skin that interfaces with the outside environment. MC precursors migrate to the skin during embryogenesis, and they develop under the influence of tissue-specific factors.[1] Although they have a well-established MC role in allergy, their relationship with hair is less understood. In fact, MCs are present in lesions of patients with alopecia areata,[2] and patients with alopecia areata frequently report itching during the activity phase of the disease. Interestingly, MC hyperplasia is a striking feature of hairless mice discovered by Fujii et al.[3] However, the mechanisms of this MC hyperplasia in hairless mice were not investigated further. Genetically, hairless mice are characterized by the absence of the hairless gene *(Hr)*.

Hr is highly expressed in both human and mouse skin. Degrading *Hr* mRNA results in transformation from hairy skin into hairless skin. However, MC hyperplasia observed in the skin of hairless mice is not a distinctive feature of *Hr* mutant mice. In fact, an increased number of MCs in the skin was reported in different strains of hairless mice, including BALB/c nude mice, a strain of mice with the absence of thymus but a normal *Hr* gene.[4] Moreover, a previous study noted that MC numbers increased during the period when hair regeneration enters late anagen, suggesting that MC numbers can oscillate with environmental changes during the hair growth cycle.[5]

One main characteristic of absent hair is thought to be the physical feature of habitats for a distinctive microbiome on the skin surface. Our group recently demonstrated that the microbiome induces MC maturation in the skin because it induces stem cell factor (SCF) production in keratinocytes, which is essential for MC survival.[6,7] Therefore we hypothesized that changes in the skin microbiome caused by hair loss could be an important factor in increasing the number of MCs present in the skin of hairless mice.

We first generated C57 HR (C57BL/6J hairless) mice, which present with MC hyperplasia and hairless skin compared with the hairy skin of C57 wild-type (WT) mice. We evaluated the number of MCs in the skin and found a significant increase in MC numbers by counting MCs from 5 tissue sections of 4 mice per group. The average number of MCs in the C57 WT group was $24 \pm 4/mm^2$, whereas that in C57 HR mice was $83 \pm 16/mm^2$ (Fig 1, *A-C*). Interestingly, C57 HR newborn mice have normal first fur, but pups start losing hair from the 14th day after birth.

Therefore, to determine whether the discontinued hair cycle affects MCs, we verified MC numbers in hairy skin from 1-week-old (1WO) C57 HR mice by means of avidin staining. As expected, we found that the average number of MCs in the 1WO C57 HR group was 51 ± 3 MCs/mm^2, which was less than the average 85 ± 7 MCs/mm^2 in adult skin of C57 HR mice (Fig 1, *D-F*, and see Fig E1 in this article's Online Repository at www.jacionline.org). When we compared 1WO C57 WT mice with 8-week-old mice, they had slightly fewer MCs. However, 1-week-old C57 mice WT already had a significantly lower number of MCs when compared with the 1WO C57 HR mice. This difference could be considered the genetic component of HR mice for MC numbers.

To assess the function of MCs in C57 HR mice, we examined MC-specific enzyme activities, such as chymase and tryptase. Immunofluorescent staining showed that there was an increased expression of chymase in C57 HR mice that correlated with the accumulation of excessive MCs in their dermis (Fig 1, *G-J*). A remarkably high β_2-tryptase *(Tpsb2)* expression was found in the skin of C57 HR but not C57 WT mice (Fig 1, *K*). Likewise, a strikingly high expression of trypsin-like activity was found when we performed fluorometric analysis (Fig 1, *L*). In addition, we evaluated MC function by measuring the diameter increase in skin edema using Compound 48/80 (Sigma, St Louis, Mo). We found that C57 HR mice had a much bigger edema area than C57 WT mice, which indicated increased release of MC mediators (Fig 1, *M*).

We also measured MC reactivity using passive cutaneous anaphylaxis. A larger edema area was observed in C57 HR mice, suggesting MCs were activated by IgE (Fig 1, *N*). These results demonstrate that MCs in skin of C57 HR mice are functioning normally.

Given that our laboratory previously demonstrated that MC maturation and migration can be promoted by using skin commensal gram-positive bacteria through the Toll-like receptor 2 (TLR2)–SCF pathway in keratinocytes,[6,7] we investigated the composition of the skin microbiome in C57 HR and C57 WT mice. Skin microbiome composition was assessed by using 16S rRNA sequencing performed on 14 samples, including 8 C57 WT mice, 4 C57 HR mice, and two 1-week-old C57 HR mice.

METHODS

Clinical subjects

Patients with IPEX were included from Italy, the Unites States, and Germany. All patients fulfilled clinical diagnostic criteria for IPEX, requiring a disruptive *FOXP3* mutation and manifestation of enteropathy and/or endocrinopathies. Blood donors not known to suffer from autoimmune disease were included as healthy controls, both in the discovery (n = 24) and in the validation control (n = 75) groups. The validation control groups also included additional subjects with autoimmune diseases: 20 subjects with autoimmune polyendocrine syndrome type 1 (APS1); 20 subjects with APS2 *with* type 1 diabetes; 20 subjects with APS2 *without* type 1 diabetes; 10 subjects with ulcerative colitis; and 10 subjects with Crohn disease.

Protein array screening

Protein arrays containing more than 9000 full-length human proteins (ProtoArray v5.1, PAH05251020, ThermoFisher, Waltham, Mass) were used to study autoantibodies in serum samples diluted 1:2000. The arrays were probed according to the manufacturer's protocol using the recommended reagents: (PA055, ThermoFisher), Alexa Fluor 647 goat antihuman IgG (A21445, ThermoFisher), Dylight 550 goat anti-GST (#DY550011-13-001, Cayman Chemicals, Ann Arbor, Mich), and the LuxScan HT24 (BioCapital) micro-array scanner.

Radio-ligand binding assay

Autoantibodies were measured by immunoprecipitation of antigens radiolabeled with ^{35}S-methionine. Complementary DNA clones were purchased from Origene and subcloned into pTNT or Sp64 expression vectors (L5610, Promega, Madison, Wis), which were used for transcription and translation *in vitro* (Promega TNT Systems): USH1C SC336653 (NM_001297764), ANKS4B SC306281 (NM_145865), HNF4A SC307232 (NM_178849), PPARG SC322218 (NM_138712), RXRA SC118299 (NM_002957), VIL1 SC123608 (BC_017303). Immunoprecipitation was conducted in 96-well filtration plates (Millipore, Burlington, Mass). Serum samples (2.5 μL) were incubated overnight at 4°C with 30'000 cpm of radiolabeled protein. Immune complexes were captured with protein A Sepharose (Protein A Sepharose 4 Fast Flow, GE Healthcare, Chicago, Ill) during a 45-minute incubation. After 10 washing steps, radioactive decay was measured in a beta counter (1450 Microbeta Triplex, Wallac). All serum samples were tested in duplicate in separate wells. BSA (4%) was included in each plate to serve as a negative standard. For each antigen, a selected IPEX or APS1 patient serum was included in all 96-well plates to serve as a positive standard for index calculation. Autoantibody indices were calculated according to the following: (sample value − negative standard value) ÷ (positive standard value − negative standard value) × 100. The upper limits of the normal range were defined as an index value of 5 SDs above the mean of the healthy controls.

Statistics

Quantile normalization was applied to reduce the effects of technical variation between different protein array experiments.[E1] Protein targets affected by printing contaminations were identified using a previously described approach and removed (n = 4).[E2] Protein targets were sorted by their difference between cases and controls. For each protein, the strongest signal intensity in the control group was subtracted from the second to strongest patient signal intensity. Thereby, targets with elevated signal in 2 or more patients could be selected. Clusters of autoantigens were identified by correlation.

Study approval

All study subjects gave their informed consent for participation in accordance with their local institutional review boards (IRBs). The study was performed in accordance with the Declaration of Helsinki and approved by the local ethics committees (2008/296-31/2 and 2016/2553-31/2 by Stockholm, UP 00-052 by Uppsala, IRB protocol TIGET02 and TIGET06 by Ospedale San Raffaele, and IRB protocol 34131 by Stanford University).

Protein annotation

The STRING database was used for functional enrichment analysis of PFAM protein domains, and GO-terms describing biological processes.[E3] Protein primary structures retrieved from the array manufacturer were aligned with Clustal omega.[E4,E5] Mutations were annotated using the gene transcript hg19_knownGene_uc004dnf.4, chrX:49106897-49121288.

Protein expression levels and immunohistochemistry

RNA-Seq data from the GTEx database were used to investigate protein expression.[E6-E8] To detail the tissue distribution of novel autoantigens, we investigated immunohistochemical stainings retrieved from the Human Protein Atlas.[E9,E10]

We thank the *Autoimmunity Profiling* National Facility in Stockholm, Science for Life Laboratory, for excellent technical assistance.

REFERENCES

E1. Bolstad BM, Irizarry RA, Astrand M, Speed TP. A comparison of normalization methods for high density oligonucleotide array data based on variance and bias. Bioinformatics 2003;19:185-93.
E2. Landegren N, Sharon D, Freyhult E, Hallgren A, Eriksson D, Edqvist PH, et al. Proteome-wide survey of the autoimmune target repertoire in autoimmune polyendocrine syndrome type 1. Sci Rep 2016;6:20104.
E3. Szklarczyk D, Morris JH, Cook H, Kuhn M, Wyder S, Simonovic M, et al. The STRING database in 2017: quality-controlled protein-protein association networks, made broadly accessible. Nucleic Acids Res 2017;45:D362-8.
E4. Goujon M, McWilliam H, Li W, Valentin F, Squizzato S, Paern J, et al. A new bioinformatics analysis tools framework at EMBL-EBI. Nucleic Acids Res 2010;38:W695-9.
E5. Sievers F, Wilm A, Dineen D, Gibson TJ, Karplus K, Li W, et al. Fast, scalable generation of high-quality protein multiple sequence alignments using Clustal Omega. Mol Syst Biol 2011;7:539.
E6. Carithers LJ, Ardlie K, Barcus M, Branton PA, Britton A, Buia SA, et al. A novel approach to high-quality postmortem tissue procurement: The GTEx Project. Biopreserv Biobank 2015;13:311-9.
E7. Lonsdale J, Thomas J, Salvatore M, Phillips R, Lo E, Shad S, et al. The Genotype-Tissue Expression (GTEx) project. Nat Genet 2013;45:580.
E8. Available at: www.gtexportal.org. Accessed August 22, 2017.
E9. Available at: www.proteinatlas.org. Accessed February 15, 2018.
E10. Uhlen M, Fagerberg L, Hallstrom BM, Lindskog C, Oksvold P, Mardinoglu A, et al. Proteomics. Tissue-based map of the human proteome. Science 2015;347:1260419.

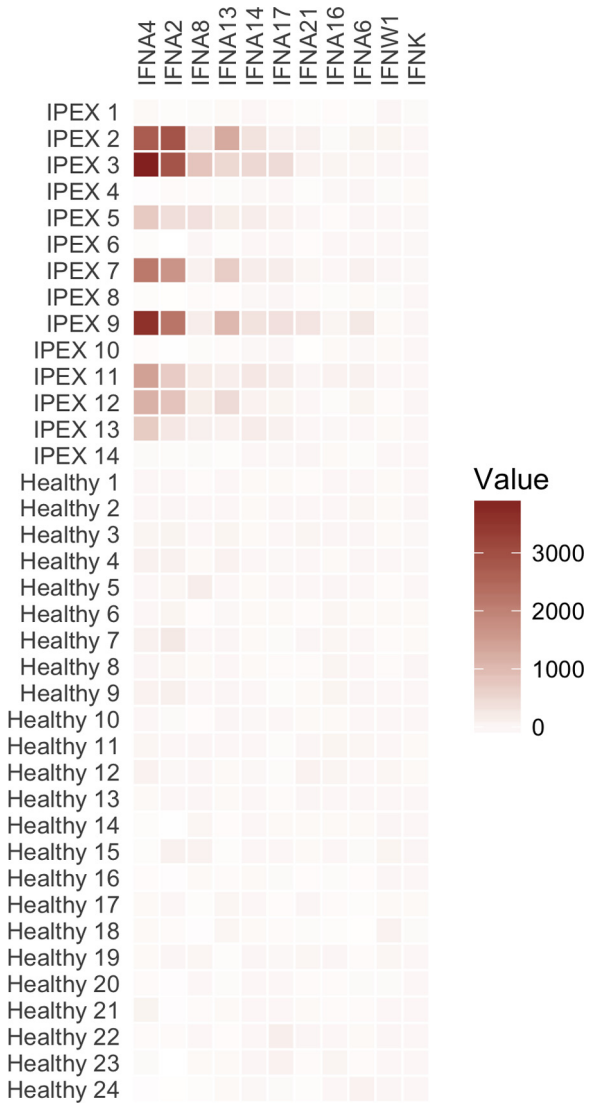

FIG E1. Protein array signal intensities for α-IFNs. Heatmap of signal intensities in 14 patients with IPEX and 24 healthy controls for IFNs present on the protein array. Samples reactive with α-IFNs are exclusively patients with IPEX.

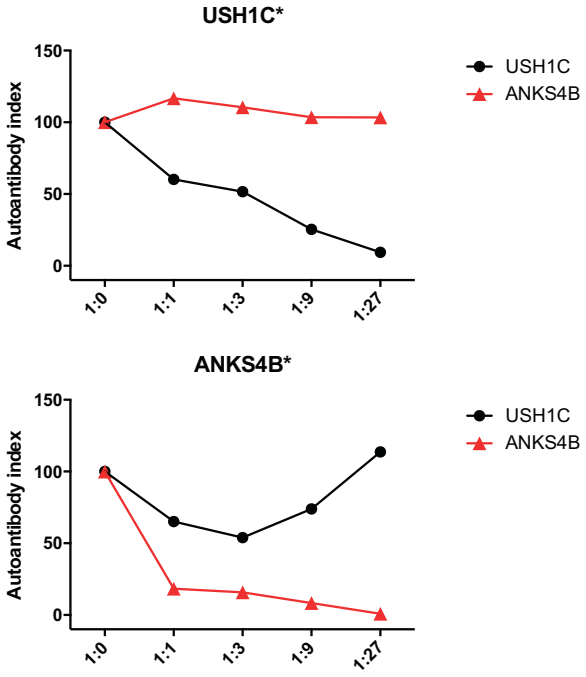

FIG E2. Competition assays for USH1C and ANKS4B. USH1C and ANKS4B autoantibodies were tested for cross-reactivity. Radio-ligand binding assays were performed in presence of increasing amounts of unlabeled protein. Radiolabeled antigens (*) were competed against unlabeled protein. The x-axes denote the ratios of labeled to unlabeled protein. No competition was observed, suggesting that USH1C and ANKS4B were independent antigens.

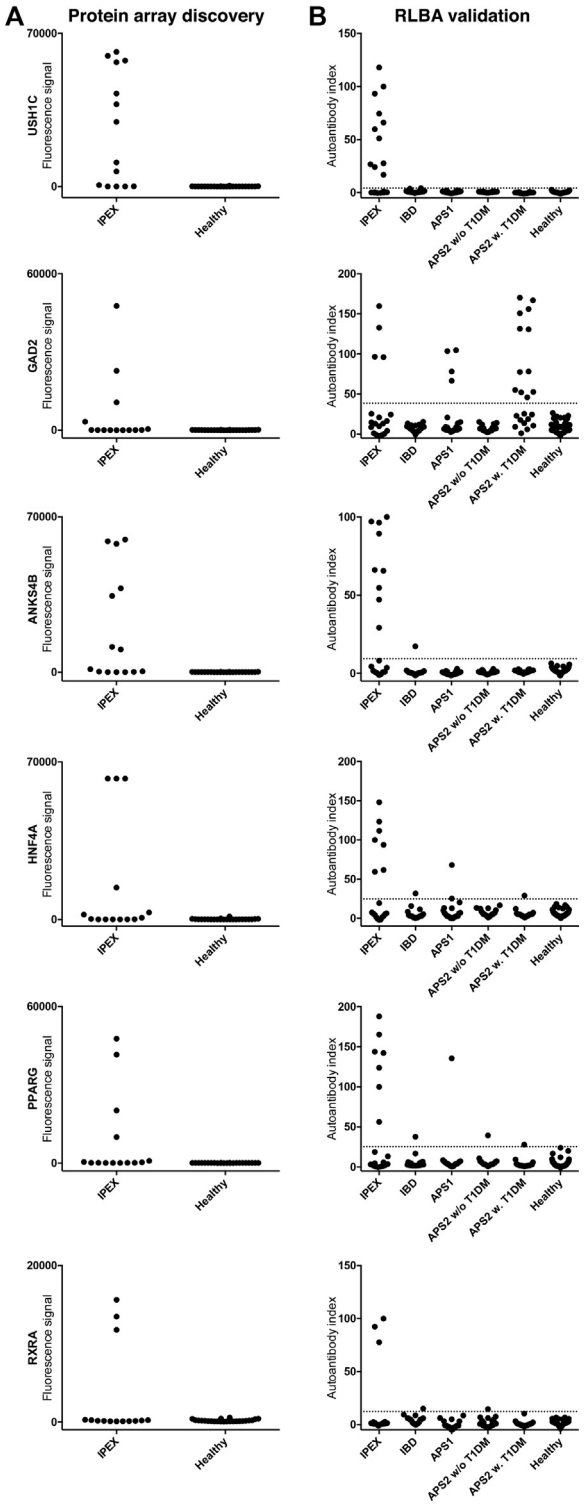

FIG E3. Verification of novel autoantigens with independent methods in extended case and control groups. The previously identified autoantigens harmonin (USH1C) and glutamate decarboxylase-65 (GAD2), and the novel candidate autoantigens harmonin-interacting protein (ANKS4B), HNF4A, RXRA, and PPARG, showed elevated signals in the protein array screening **(A)**, and were validated using radio-ligand binding assays **(B)**. All 14 patients with IPEX from the discovery screen and 3 new patients with IPEX were assessed. Additional control subjects were included: 75 healthy blood donors; 20 subjects with APS1; 40 subjects with APS2 (10 with and 10 without type 1 diabetes mellitus); and 20 subjects with inflammatory bowel disease (10 with ulcerative colitis and 10 with Crohn disease).

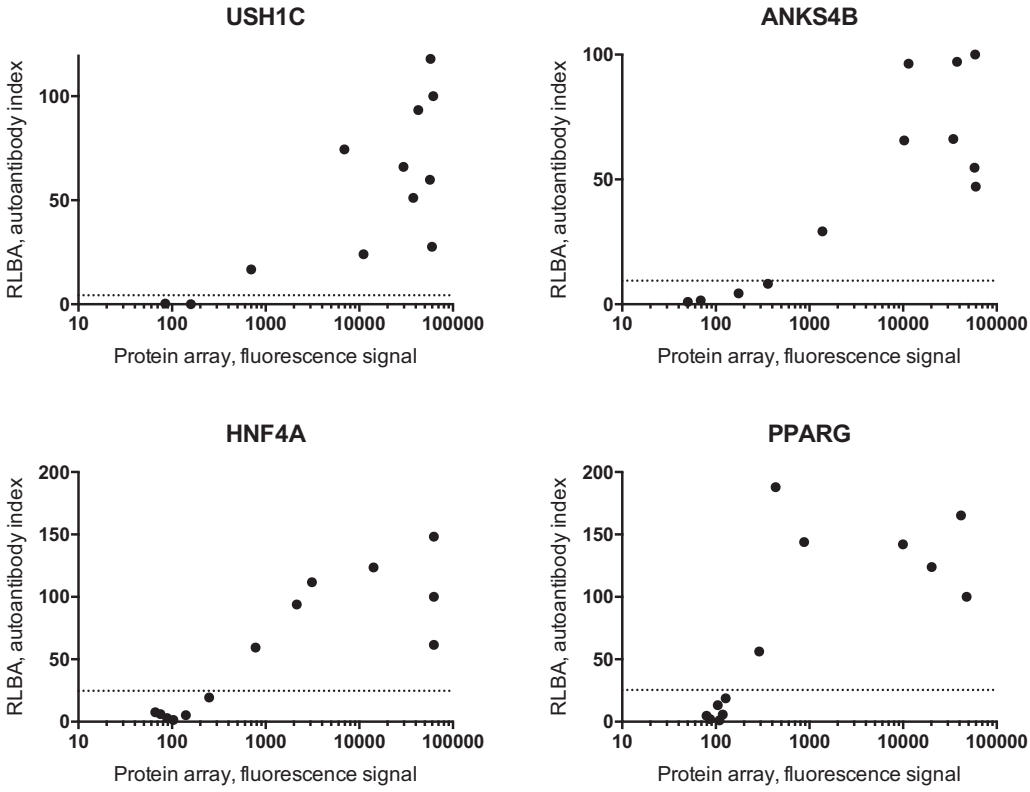

FIG E4. Comparison of protein array and RLBA results. Patients with IPEX who had weakly elevated signals in the protein array screen came out positive in the validation experiments using the sensitive radio-ligand binding assays. The x-axes display the fluorescence signal intensities detected in the protein array experiment on a logarithmic scale. The y-axes display autoantibody index from the RLBAs. Each data point represents a patient with IPEX (n = 14). *Dotted lines* mark the cutoff levels for the RLBAs. *RLBA,* Radio-ligand binding assay.

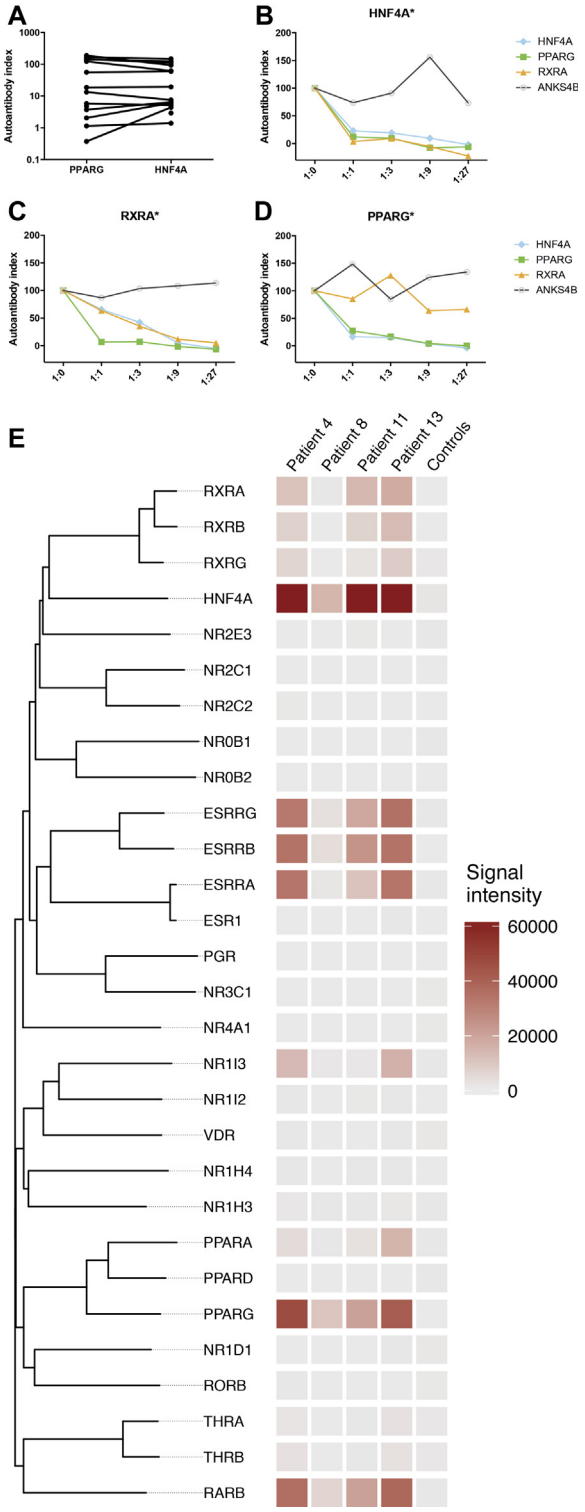

FIG E5. Nuclear receptor autoantibodies target a shared epitope in the ligand-binding domain. **A,** The RLBA results for PPARG and HNF4A autoantibodies were similar. Results from single patients with IPEX are connected with lines (n = 14). **B-D,** Competition assays were used to study autoantibody cross-reactivity. Radiolabeled nuclear receptor autoantigens (*) were competed against unlabeled protein of the same autoantigen species, other nuclear receptor autoantigens, and ANKS4B as a negative control. The x-axes denote ratios of labeled to unlabeled protein. **E,** The heatmap displays signal intensities for the nuclear receptors in the protein array ordered by sequence similarity. The 4 patients with IPEX with the strongest signals for nuclear receptor autoantigens are included. The strongest signal among healthy controls has been summarized in 1 column, to illustrate that all healthy controls had weak signals for all nuclear receptors. *RLBA*, Radioligand binding assay.

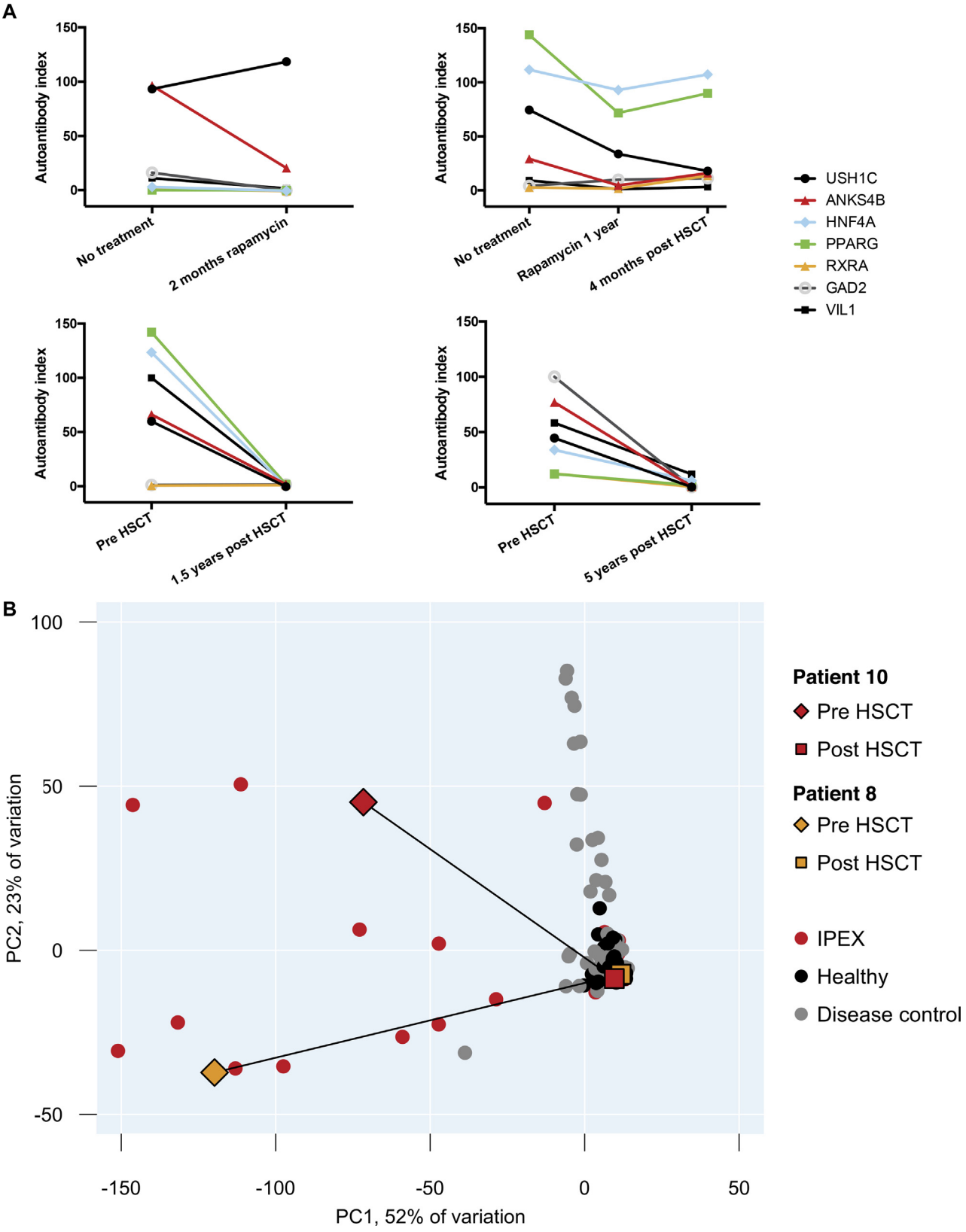

FIG E6. Autoantibodies are undetectable following allogenic HSCT. **A,** The autoantibody profiles detected in consecutive samples from 4 patients with IPEX undergoing immunosuppressive treatment and/or HSCT. Each subpanel includes data from a single patient. Complete normalization of autoantibody levels was seen 1.5 years and 5 years after HSCT. **B,** A principle component (PC) space calculated from RLBA results. The investigated patient and control samples are indicated with *dots*. Patients sampled before *(diamonds)* and after *(squares)* HSCT moved *(connecting lines)* away from the scattered cluster of patients with IPEX (red) to the cluster of healthy controls (black), as autoantibodies became undetectable. *RLBA,* Radioligand binding assay.

TABLE E1. Clinical and genetic characteristics of patients with IPEX syndrome

Patient	Age at sampling	Enteropathy	T1DM	Dermatitis	Additional diagnoses	*FOXP3* mutation
1	0 y	Yes, 1 mo	No	Yes, 1 mo	Autoimmune hepatitis; nephrotic range proteinuria, hematuria	c.1270_1272delinsC (p.C424L-fs*34)
2	28 y	Yes, 5 mo	No	Yes, 5 mo	Arthritis; ITP; renal cell carcinoma; lymphoma	c.816+2 T del (splice donor variant)
3	10 y	Gastritis, 8 y	No	No	Low-molecular-weight proteinuria	c.210+1 G>C (splice donor variant)
4	10 y	Yes, 4 mo	Yes, birth	Yes, birth	AIHA; thrombocytopenia	c. 1040 G>A (p.R347H) (FKH dom)
5	3 y	Yes, 1 mo	No	No	None	c.750-752del (p.E250del)
6	5 mo	Yes, 1 mo	Yes, birth	No	None	c.736-1 G>A (splice acceptor site)
7	17 y	Yes, 2 mo	No	No	None	c.1222 G>A (p.V408M)
8	1 y	Yes, 6 mo	Yes, 10 d	Yes, 3 mo	None	c.1117 TT>GC (p.F373A) (FKH dom)
9	18 y	Yes, 1 mo	Yes, 2 y	Yes, 1 mo	AIHA; alopecia; autoimmune thyroiditis; arthritis	c.1150 G>A (p.A384T) (FKH dom)
10	6 y	Yes, 40 d	No	Yes, 40 d	AIHA; lymphadenopathy; CMV hepatitis	c.1078 C>T (p.L360F)
11	3 y	Yes, 2 y	No	No	None	c.1190 G>A (p.R397Q)
12	28 y	Yes, 7 mo	Yes, 18 y	Yes, 18 y	Hepatitis	c.1040 G>A (p.R347H)
13	1 y	Yes, 3 mo	Yes, 2 w	Yes, 1 mo	Autoimmune thyroiditis; neurodevelopmental delay; hepatitis	c.210+2 T>G (splice donor variant)
14	1 y	No	Yes, 10 mo	No	None	c.210+2 T>G (splice donor variant)
15	27 y	Yes, 3 mo	Yes	Yes	None	c.1150 G>A (p.A384T) (FKH dom)
16	1 y	Yes, 4 mo	No	Yes, 2 mo	None	c.816+5C>T (splice donor variant)
17	3 y	Yes, 2 mo	No	Yes, 3 mo	AIHA	c.751-753delGAG (p.Glu251del)

AIHA, Autoimmune hemolytic anemia; *CMV*, cytomegalovirus; *FKH dom*, forkhead domain; *ITP*, immune thrombocytopenic purpura; *T1DM*, type 1 diabetes mellitus.